



January 2023

Obtaining The Transfer Function Of A Camera Mount Using Ansys And Matlab

Ikechukwu Stanley Nwade

[How does access to this work benefit you? Let us know!](#)

Follow this and additional works at: <https://commons.und.edu/theses>

Recommended Citation

Nwade, Ikechukwu Stanley, "Obtaining The Transfer Function Of A Camera Mount Using Ansys And Matlab" (2023). *Theses and Dissertations*. 5687.
<https://commons.und.edu/theses/5687>

This Thesis is brought to you for free and open access by the Theses, Dissertations, and Senior Projects at UND Scholarly Commons. It has been accepted for inclusion in Theses and Dissertations by an authorized administrator of UND Scholarly Commons. For more information, please contact und.common@library.und.edu.

**OBTAINING THE TRANSFER FUNCTION OF A CAMERA MOUNT USING
ANSYS AND MATLAB.**

by

Ikechukwu Stanley Nwade

A Thesis

Submitted to the Graduate Faculty

Of the

University of North Dakota

in partial fulfilment of the requirements

for the degree of

Master of Science

Grand Forks, North Dakota

December

2023

This thesis, submitted by Nwade Ikechukwu Stanley in partial fulfilment of the requirements for the Degree of Master of Science from the University of North Dakota, has been read by the Faculty Advisory Committee under whom the work has been done and is hereby approved.

Neubert Jeremiah, Chair

Semke William

Tang Clement

This thesis is being submitted by the appointed advisory Committee as having met all the requirements of the School of Graduate Studies at the University of North Dakota and is hereby approved.

Chris Nelson
Dean of the School of Graduate Studies

Date

PERMISSION

Title: Obtaining the transfer function of a camera mount using ANSYS and MATLAB.

Department: Mechanical Engineering

Degree: Master of Science

In presenting this thesis in partial fulfillment of the requirements for a graduate degree from the University of North Dakota, I agree that the library of this University shall make it freely available for inspection. I further agree that permission for extensive copying for scholarly purposes may be granted by the professor who supervised my thesis work or his absence, by the Chairperson of the department or the dean of the School of Graduate Studies. It is understood that any copying or publication or other use of this thesis or part thereof for financial gain shall not be allowed without my written permission. It is also understood that due recognition shall be given to me and to the University of North Dakota in any scholarly use which may be made of any material in my thesis.

Nwade Ikechukwu Stanley

5th Dec 2023

TABLE OF CONTENTS

LIST OF FIGURES	vi
LIST OF TABLES.....	viii
ACKNOWLEDGEMENTS.....	ix
ABSTRACT.....	x
CHAPTERS	
1. INTRODUCTION	1
2. LITERATURE REVIEW.....	5
2.1. Overview of Augmented Reality.....	5
2.2. Transfer Function in Camera Stability.....	6
2.3. Transfer Function Using ANSYS and MATLAB.....	7
2.4. Challenges and Future Directions.....	10
3. METHODOLOGY.....	12
3.1. Theoretical response of the structure to base excitation.....	12
3.2. Validate the transient response from ANSYS with that of the theoretical response.....	15
3.3. Harmonic analysis in ANSYS to get the frequency response function.....	19
3.4. Generate the transfer function based on the Frequency Response Function (FRF) from ANSYS.....	21

3.5. Validate the transfer function by comparing the simulated response to the validated response.....	21
4. RESULTS AND DISCUSSION.....	23
4.1. Mesh Quality.....	24
4.2. Frequency Response Function of the Camera Mount.....	26
4.3. Deriving the Transfer Function using System Identification Toolbox in MATLAB.....	26
4.4. Validation of Derived Transfer Function of Camera Mount.....	27
5. CONCLUSIONS AND RECOMENDATION.....	30
6. APPENDIX A	32
7. APPENDIX B	37
REFERENCES	39

LIST OF FIGURES

Figure 1a: Application of the HUD.....	1
Figure 1b: Multiple views of the camera mount (unit inches).....	2
Figure 2: Typical cantilever beam with tip-mass.....	13
Figure 3: The first five mode shapes of the cantilever beam with tip mass.....	14
Figure 4: Transient structural analysis settings.....	17
Figure 5: Transient structural displacement settings.....	17
Figure 6: The analysis settings of the harmonic response.....	20
Figure 7: Frequency response plot at tip-mass due to base excitation.....	21
Figure 8: Plot showing the predicted and validation response of the cantilever beam with tip-mass.....	22
Figure 9: Position of the camera on the camera mount.....	23
Figure 10: Meshing of the camera mount.....	24
Figure 11: Comparison of the transient responses between two different mesh sizes.....	25
Figure 12: The first mode shape at 325.99Hz.....	25
Figure 13: FRF plot at the camera position.....	26
Figure 14: Comparison between FRF transfer function and ANSYS transient simulation (Displacement is 2mm, 10Hz).....	27

Figure 15: Comparison between FRF transfer function and ANSYS transient simulation (Displacement is 10mm, 10Hz).....	28
Figure 16: Comparison between FRF transfer function and ANSYS transient simulation (Displacement is 10mm, $\omega = 5\text{Hz}$).....	28
Figure 17: Comparison between FRF transfer function and ANSYS transient simulation (Displacement is 2mm, frequency is 5Hz).....	29

LIST OF TABLES

Table 1: Characteristics of the cantilever beam including tip-mass.....	15
Table 2: comparison of the first -five natural frequencies from Ansys and analytical.....	15
Table 3: Mode shapes from ANSYS.....	16
Table 4: Tip displacement responses from transient to steady state for both theoretical and ANSYS.....	18

ACKNOWLEDGEMENTS

I would like to thank my advisor, Prof. Jeremiah Neubert, for his guidance, generous support, and patience over the course of the MSc. duration. I would also like to express my sincere appreciation to Dr. Semke William and Dr. Clement Tang for serving as my thesis committee and Dr. Djedje-Kossu Zahui for his guidance.

Special Thanks to my parents and my sisters for their continuing support, and encouragement.

ABSTRACT

In this thesis, the transfer function of a camera mount is obtained using ANSYS and MATLAB. In a heads-up display (HUD) application, achieving precise image registration requires careful consideration of the camera's position relative to the vehicle. Vibrations can alter the camera's position, with tilt being the most impactful due to its increased displacement effect as objects are further away.

This research tackles vibration by predicting the position of the camera using transfer function. To determine the transfer function for complex structures, such as camera mounts, this study aims to first establish a transfer function for a simpler model, like a cantilever beam with a tip-mass. By contrasting the transient response from ANSYS with the theoretical response of the system, the ANSYS modeling is validated as part of the process. The system identification toolbox in MATLAB is then used to produce the transfer function based on the frequency response function (FRF) that was developed in ANSYS harmonic analysis. By comparing the simulated outputs to ANSYS transient responses with the same inputs, the transfer function is verified. The results show that the transfer function developed successfully predicts the position of the camera with an accuracy of 98%.

CHAPTER 1

1. INTRODUCTION

Heads-Up Display (HUD) systems have become increasingly prevalent in automotive, aviation, and military applications, providing critical information to users while keeping their attention focused on the task at hand (Pauzie, 2015). It was observed that the duration of sustained gaze on navigational cues was noticeably reduced when utilizing the HUD, indicating a decreased amount of time dedicated to extracting information from the HUD (Ablaßmeier et al., 2007). Correspondingly, both (Kim et al., 2009) and (Medenica, Kun, Paek & Palinko, 2011) reported comparable inclinations, along with enhancements in driving performance, when employing a HUD. Notably, the latter study highlighted that 72.2% of participants expressed an improved driving experience while using the HUD. However, the performance of HUD systems can be affected by vibrations, particularly those arising from vehicle movements. These vibrations can lead to undesired displacements in the camera used for projection, resulting in misalignments and degraded display quality. Figure 1 shows the camera mount used in this thesis.



Figure 1a: Application of the HUD (Cars.com, 2023)

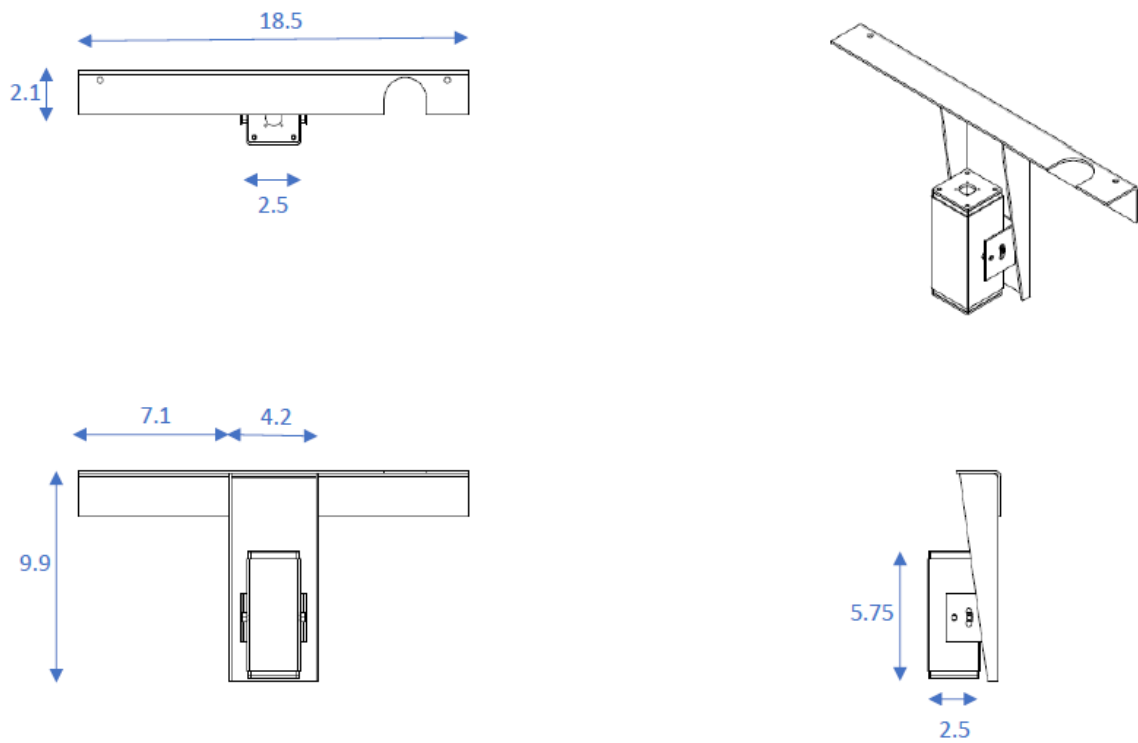


Figure 1b: Multiple views of the camera mount (unit inches)

To mitigate the effects of vibration on HUD systems, accurate prediction of the change in camera displacement is crucial. By accurately predicting these displacements, appropriate compensation techniques (Suraj, Rafael, Jussi & Aki, 2021) and (Hasegawa, Sumiyosi, Hayashi, Nishikawa, Chikuri & Tsukahara, 2019) can be employed to ensure the alignment between the projected information and the user's field of view, thus enhancing the effectiveness and usability of HUD systems. This research focuses on the design and analysis of the camera mount then the prediction of the change in camera displacement caused by vibrations to effectively mitigate their effects on HUD systems.

The literature review delves into the evolution and applications of augmented reality (AR), tracing its roots back to Thomas Preston Caudell's introduction of the term in 1992. It

highlights the wide-ranging impact of AR across industries, from entertainment to healthcare, citing its exponential growth projected to reach USD 856.2 billion by 2031. The review emphasizes the significance of accurate camera modeling and control in AR development, referencing various studies focusing on predictive control techniques, camera dynamics, and alignment between virtual and real-world objects. Transfer functions play a crucial role, demonstrated in research involving camera pose estimation, vibration management, structural analysis, and stability assessments in AR systems. Additionally, the challenges in AR technology, including calibration complexities, hardware limitations, and inaccurate depth perception, are discussed alongside the multitude of benefits transfer functions offer in AR applications, from remote control to gesture recognition and real-time rendering.

In the methodology, the research develops a method to predict the camera displacements due to vibrations. It involves understanding the dynamic behavior of the camera mount and the interaction between the camera and the vehicle. A transfer function provides a convenient representation of the input-output relationship of a linear, time-invariant system. It is derived by applying a Laplace transform to the system's differential equations, assuming the absence of initial conditions. This mathematical transformation enables a concise description of the system's dynamics in terms of its response to different inputs. Therefore, obtaining a transfer function of the system is vital for this research.

This research demonstrates a method to derive the transfer function for intricate structures, like camera mounts, by first establishing a transfer function for simpler models—such as a cantilever beam with a tip-mass. The process includes validating the ANSYS modeling by comparing the transient response against theoretical expectations. Subsequently, utilizing the Frequency Response Function (FRF) generated in ANSYS, the transfer function is created

using system identification toolbox in MATLAB. The transfer function is validated by cross-referencing the simulated outputs against ANSYS transient responses with identical inputs.

The findings of this research will contribute to the advancement of HUD systems by providing insights into predicting and mitigating the effects of vibrations on camera displacements. By improving the alignment between the projected information and the user's field of view, the proposed methods have the potential to enhance situational awareness, safety, and overall user experience in various applications.

CHAPTER 2

2. LITERATURE REVIEW

2.1 Overview of Augmented Reality

The term "augmented reality (AR)" was introduced in 1992 by Thomas Preston Caudell, a researcher at Boeing. Caudell pioneered the application of AR for industrial purposes, particularly for tasks involving assembly diagram visualization. It is an emerging technology which has uses in everything from entertainment and gaming to industry and education (Syed et al., 2022). Augmented reality (AR) stands as one of the most transformative and rapidly expanding immersive technologies in the 21st century. Its profound impact extends across various domains, encompassing healthcare, education, tourism, design, manufacturing, and several other industries. The widespread adoption of AR has propelled its growth to unparalleled heights (Sirakaya & Alsancak Sirakaya, 2022). In a recent report from September 2022, it was revealed that the combined market size of AR and virtual reality (VR) had already soared to USD 27.6 billion in 2021, and experts project that this figure will skyrocket to an astounding USD 856.2 billion by the conclusion of 2031 (Syed et al., 2022).

Accurately predicting and managing the camera's location to smoothly merge virtual items with the actual environment is one of the major hurdles in AR development. This necessitates a thorough comprehension of the behavior of the camera mount, which is possible through the derivation of its transfer function. Accurate camera modeling and control are the cornerstones of augmented reality. This issue has been the subject of extensive research. For AR applications that demand precise camera positioning, (Ligorio & Sabatini, 2015) presented a framework for camera pose estimation based on sensor fusion. Their work highlights the significance of effective camera alignment to preserve alignment between actual objects and virtual ones. The work of (Haidegger et al., 2012) is another noteworthy

contribution to the area of camera modeling and control in augmented reality. Their research explores the complexities of camera dynamics and how they affect augmented reality (AR) applications.

To account for system delays and uncertainty, the authors presented a unique camera transfer function that incorporates predictive control. This method dramatically increased the responsiveness and accuracy of AR systems, making them more appropriate for practical applications. To provide a smooth user experience, the study by (Haidegger et al., 2012) emphasizes the significance of taking camera dynamics into account and implementing predictive control techniques. In critical applications like airport operations, military training simulations, and medical scenario simulations, the need for conducting highly accurate and realistic simulations using real video imagery is paramount. This study has provided an overview of recent advancements in achieving visual realism in model construction and simulating synthetic objects seamlessly integrated into video sequences. It demonstrated how these synthetic objects can exhibit intelligent behaviors within a visually augmented reality environment (Hussain & Kaptan, 2004).

2.2 Transfer Function in Camera Stability

Transfer function is used to describe the output and input relations of the systems which can be characterized by the several factors such as time invariants, differential equations, and linear parameters. It is a valuable tool for the designing of control systems (Bozhevolnyi, Vohnsen, & Bozhevolnaya, 1999). Understanding the link between input and output in control systems begins with the derivation of transfer functions. This theory has been used by researchers to place cameras. For instance, this research has developed a transfer function for an aerial platform's camera gimbal control system. Their study shows how transfer functions can be used to forecast and manage camera orientation (Hilkert, 2008). In a research work

(Piriadarshani & Sujitha, 2018), the importance of transfer function in study of vibrations controls and camera stability of feedback control systems with delay has been investigated and analyzed the stability of feedback control systems like delayed resonators and second-order systems when controlled over a network involves employing a range of analytical methods, primarily based on transfer functions. Furthermore, this theoretical framework can be extended to encompass higher-order delay differential equations that represent complex dynamical systems (Piriadarshani & Sujitha, 2018).

In another research work (Datcu, Ibos, Candau, & Mattei, 2002), the use of transfer function in infrared camera has been calculated and analyzed to obtain heat flux emitted by surface with the help of infrared images which are mostly distorted due to the diffraction and aberration phenomena and results suggested that modulation transfer function fits well in the research and low value of fit residuals in both of the optical transfer function geometrical as well as in the diffraction optical transfer function. This study (Datcu et al., 2002) highlights the role of transfer function and its importance in the camera modelling and positioning systems.

The understanding, forecasting, and eventually controlling unnecessary vibrations in mechanical and structural systems all depend on the employment of transfer functions in vibration management. Transfer functions provide a conceptual link between the excitation forces applied at the input and the responses of the system. By quantifying how a system reacts to various frequencies, they help engineers assess and devise control schemes.

2.3 Transfer Function Using ANSYS and MATLAB

Transfer functions are, in essence, essential instruments for achieving stability and improved performance in a variety of applications, from civil engineering to aerospace. In a research work (Wu, Lei, Li, & Xie, 2013), the transfer function modelling of structural vibration of

complex aerospace structures based on finite element analysis by using ANSYS has been investigated with the idea of characterizing vibrations with the help of transfer functions for advanced control systems. This framework presented by the two domains namely time and frequency and this framework revolved around the cantilever beam, strap on launch vehicle and local parts of the aerospace structures where results indicated the selected method is effective and provided satisfactory performance for the vibration control.

An assessment of the structural dynamics of buildings and bridges, particularly their response to external elements like earthquakes and wind loads, is done in civil engineering using ANSYS (Alsaïdi et al., 2019). Another study introduced a simplified method for assessing structural vibrations in response to diverse base excitations, with a specific application focusing on railway-related issues. It takes as its input the soil excitation spectrum at the building's foundation location and calculates the structural response at any arbitrary point within its 3D framework. To demonstrate the versatility of this model, it is utilized to estimate building responses to various isolated railway irregularities, such as switches and crossings. This study concluded that this approach is novel and permits the building vibrations accounting for soil structure interaction and floor amplification (López-Mendoza, Connolly, Romero, Kouroussis, & Galvín, 2020). In another research work (Khot & Yelve, 2011), a spring-mass-damper system with two degrees of freedom have been considered. The results of its FE model's modal analysis performed in ANSYS were used to create its state space mathematical model in the primary coordinate system in MATLAB. Transfer function and state space model in physical coordinates of the same system are mathematically developed under the assumption of proportional damping to verify the model's validity. All the system models' frequency responses are compared and found to be in good agreement. The system model of a cantilever beam is also retrieved in MATLAB from the results of the modal analysis of its FE model in ANSYS, and its frequency response is presented to show the application of this study. In

ANSYS and MATLAB, the cantilever beam's response to a unit impulse input has been also obtained and found satisfactory this concludes the ease transfer functions can offer using MATLAB and ANSYS for the real time applications of vibrational analysis. Transfer functions enable the modeling, analysis, and optimization of complex systems spanning numerous engineering disciplines in both MATLAB and ANSYS. They offer a potent tool for comprehending system behavior and making wise design and control choices.

Researchers (Friedrich, Brauers, Bell, & Aach, 2010) have investigated techniques for measuring and assuring system stability, which is essential for camera positioning in augmented reality applications. These researchers conducted stability analysis for camera control in autonomous robotic systems, which has implications for augmented reality camera systems. Another research work (Sarwar & Malik, 2010) focused on the stability analysis and simulation of a two-degree-of-freedom (2-DOF) robotic system designed for precise device positioning and aiming. The system is based on a linear model and is constructed by integrating both a tilt mechanism and a pan mechanism. Before developing the motion controllers for this 2-DOF robotic system, a thorough stability analysis of the pan and tilt mechanisms is conducted. This is concluded that this analysis serves as a crucial preliminary step in the design process. It involved establishing the state space model and transfer functions for both the pan and tilt mechanisms to provide a comprehensive understanding of their behavior.

The FRF is typically depicted as a complicated function, the magnitude and phase of which offer information about the system's behaviour at different frequencies (Radeş, 2001).

By examining the FRF data, transfer functions may be extracted, providing a way to understand the dynamics of the system's reaction to various inputs.

Transfer functions have several applications in the augmented reality as these transfer functions have been used for the calibration of cameras in AR technology by modelling of the relationship between real world and view of camera and helps in the correction of disturbances and aligns virtual objects (Lepetit, Vacchetti, Thalmann, & Fua, 2003). Transfer functions have also been involved in the depth sensing techniques such as structure light. These are also used in object tracking and can provide motion and behavior of tracked objects. Instead of the numerous benefits such as remote control, increased marketing, reduction in development time, gesture recognition, physics simulations, real time tendering and others that have been offered by the transfer functions in AR technology there are several challenges in its usage in the AR applications which involve complexities in calibration, variable environment, inaccurate perception of depth, hardware limitations, adoption development costs and others (Chu, Matthews, & Love, 2018).

2.4 Challenges and Future Directions

Despite its diversity and strength, using ANSYS and MATLAB has its share of difficulties and restrictions. Both software programmes can be difficult to operate, especially for new users, and require time and instruction. Their price may be too high for smaller businesses and people, which would restrict accessibility. High-performance hardware is often required to do simulations and analysis in ANSYS and MATLAB since they might be computationally taxing. It can be difficult to integrate these tools with other programmes or systems, and it can be necessary to design a custom solution. The quality of the input data, which can be difficult to ensure, has a significant impact on how accurate the outcomes are. Model validation against real-world data is frequently challenging and time-consuming, potentially producing inaccurate results. Organizations may struggle with managing licenses and making sure software usage agreements are followed (Mendoza-Ramírez et al., 2023).

Future advancements might concentrate on making these tools more user-friendly in order to increase their accessibility to a wider variety of consumers. Versions of ANSYS and MATLAB that are hosted in the cloud can improve accessibility and lower system requirements: (Warren, 2014). The creation of open-source alternatives might give users and researchers affordable choices Prasad (Prasad Mohanty & Goswami, 2021).

CHAPTER 3

3. METHODOLOGY

The development of a transfer function in this paper follows a certain methodology which is shown on a cantilever with tip-mass first before implementing on a more complex structure as my camera mount. The cantilever with tip-mass is used to understand the process of extracting a good harmonic FRF and transient response from ANSYS.

The Steps taken involves:

1. Theoretical response of the structure to base excitation.
2. Validate the transient response from ANSYS with that of the theoretical response.
3. Harmonic analysis in ANSYS to get the frequency response function.
4. Generate the transfer function by utilizing the System Identification Toolbox in MATLAB, based on the Frequency Response Function (FRF) from ANSYS.
5. Validate the transfer function by comparing the simulated response to the validated response.

3.1. Theoretical response of the structure to base excitation

The camera mount is simplified to the schematic diagram in figure 2 which illustrates a uniform cantilever beam subjected to base excitation, with a tip-mass attached at the free end. It is important to note that while the gravity center of the tip-mass is aligned with the gravity center of the beam, it does not coincide with the point of attachment at the end, denoted as o' . Both the mass and the moment of inertia of the tip-mass are considered, whereas the rotary inertia of the beam is disregarded.

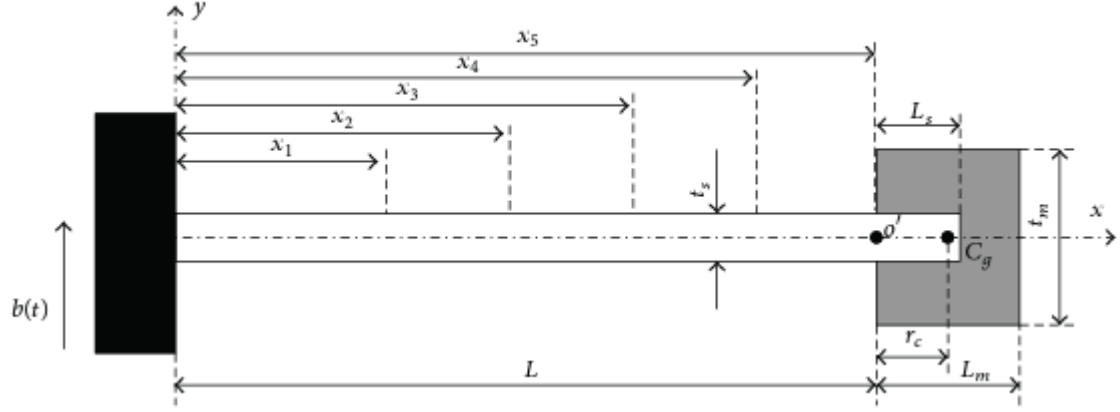


Figure 2: Typical cantilever beam with tip-mass

The characteristic equation and mode shape of the structure is given by (Wang, Qingfeng, & Wuwei, 2014).

$$1 + cch - \phi u(sch - csh) - R_1[sch + csh - \phi u(1 - cch)] - 2R_2ssh - R_2^2(1 - cch) = 0, \quad (1)$$

$$U_i^3(x) = \sin\left(\frac{u_i x}{L}\right) - sh\left(\frac{u_i x}{L}\right) - \lambda \left[\cos\left(\frac{u_i x}{L}\right) - ch\left(\frac{u_i x}{L}\right) \right] \quad (2)$$

Where $\lambda = A_{12}/A_{11}$ and $A_{11} = -(1 + R_2)c + (R_2 - 1)ch + R_1(s + sh)$,

$$A_{12} = R_1(ch - c) - (1 + R_2)s + (R_2 - 1)sh,$$

$$u = \beta L, \quad s = \sin(u), \quad c = \cos(u), \quad sh = \sinh(u), \quad ch = \cosh(u),$$

$$\phi = M/(mL), \quad R_1 = \phi u^3 \left[\left(\frac{K}{L}\right)^2 + \left(\frac{r_c}{L}\right) \right], \quad R_2 = \phi u^2 \left(\frac{r_c}{L}\right), \quad K = \sqrt{J/M}$$

The natural frequencies are gotten from the first five roots of the characteristic equation (1)

u_1 to u_5 as $w_1 = 81.5$ Hz, $w_2 = 912.4$ Hz, $w_3 = 2.478 \times 10^3$ Hz, $w_4 = 5.3576 \times 10^3$ Hz and $w_5 = 9.9459 \times 10^3$ Hz.

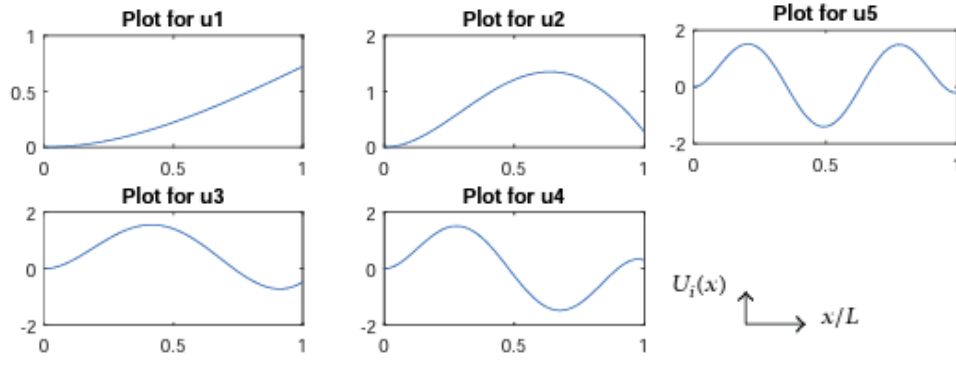


Figure 3: The first five mode shapes of the cantilever beam with tip mass

The absolute displacement response of the cantilever beam with tip-mass under base transverse excitation can be obtained as

$$u_a(x, w, t) = \sum_{i=1}^{\infty} \{ U_{iN}^{(k)}(x) \frac{B[MU_{iN}^{(k)}(L) - r_c M \left(\frac{dU_{iN}^{(k)}(L)}{dx} \right) - m \int_0^L U_{iN}^{(k)}(x) dx]}{\sqrt{w^4 + 2(2\zeta^2 - 1)w^2 w_i^2 + w_i^4}} \times \left[\frac{w^3}{w_i \sqrt{1 - \zeta^2}} e^{-w_1 \zeta t} \sin(w_i \sqrt{1 - \zeta^2} t + \phi_1) + w^2 \sin(wt + \phi_2) \right] \} \quad (3)$$

Where U_{iN} is the normalized mode shapes, B chosen to be 0.01mm is the amplitude of the input sine-displacement excitation, w is the excitation frequency of the base displacement, ζ is the damping ratio found to be 0.0025 by Logarithmic Decrement Method. Where ϕ_1 and ϕ_2 are determined by $\tan(\phi_1) = 2\zeta\sqrt{1 - \zeta^2} / ((w/w_i)^2 + 2\zeta^2 - 1)$ and $\tan(\phi_2) = -2\zeta(w/w_i) / (1 - (w/w_i)^2)$.

The solution includes two components with respect to time. The first term corresponds to free vibration, which gradually decays over time in an exponential manner. The second term, influenced by the excitation, represents the forced vibration of the system. The equation was verified experimentally by the authors.

Physical properties	Beam	Tip-mass
Young's modulus, E (GPa)	69	—
Density, ρ_s or ρ_m (kg/m ³)	2630	7753
Length, L or L_m (mm)	120.4	15.6
Thickness, t_s or t_m (mm)	4.9	29.5
Width, w (mm)	10.2	10.2
Total mass, M (g) ^a	—	33.83
Offset, r_c (mm) ^b	—	8.01
Rotary inertia, J (kg·m ²) ^{b,c}	—	3.33×10^{-6}

Table 1: Characteristics of the cantilever beam including tip-mass

3.2. Validate the response from ANSYS with that of the theoretical response.

Finite element and experimental analysis have always been used to verify a mathematical model in the field of engineering. Ansys, a powerful engineering simulation software, was used for this analysis. Modal analysis is a technique used to study the dynamic behavior of a structure or system. It focuses on the vibration characteristics and natural modes of oscillation exhibited without an external force. The system in figure 2 is modeled with the parameters found in table 1 such that the end of the beam attached to the base is fixed and the first five natural frequencies and mode shapes are obtained along y axis. When modeling the cantilever beam with tip-mass, I adjusted the density and volume to match the tip-mass of 33.83g for the beam since the material was not found in ANSYS.

Approach	w_1	w_2	w_3	w_4	w_5
Analytical	81.5	912.4	2479	5357.6	9945.9
ANSYS	82.1	925.53	2486.7	5259	9573.7
% Error	0.74%	1.43%	0.31%	1.84%	3.74%

Table 2: comparison of the first -five natural frequencies from Ansys and analytical

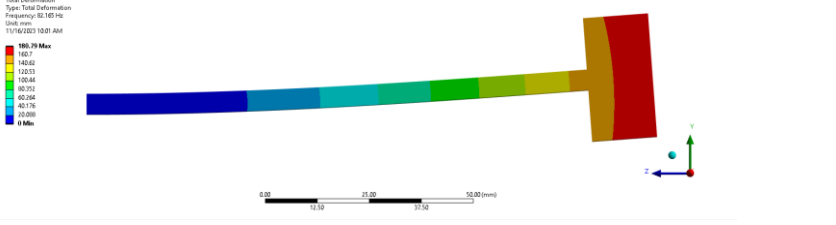
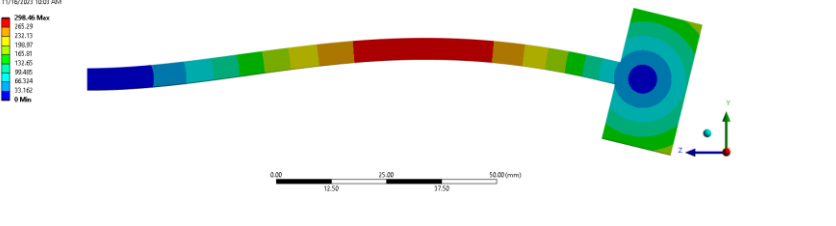
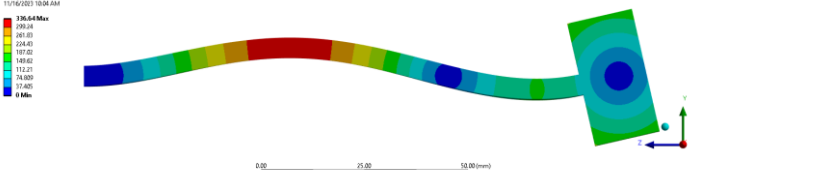
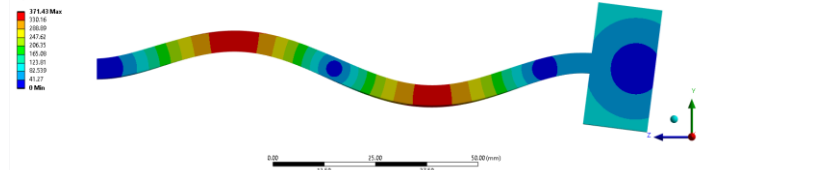
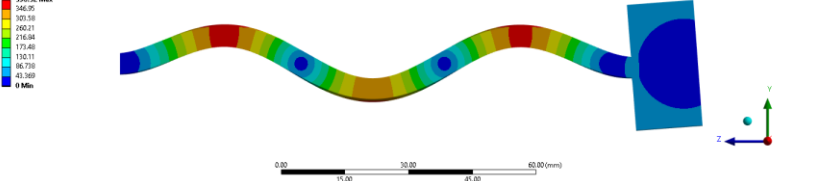
Frequency	Mode shape
W_1	<p>C: Modal test2 Total Deformation Type: Total Deformation Frequency: 62.165 Hz Unit: mm 11/16/2023 10:01 AM</p> 
W_2	<p>C: Modal test2 Total Deformation 2 Type: Total Deformation Frequency: 95.133 Hz Unit: mm 11/16/2023 10:03 AM</p> 
W_3	<p>C: Modal test2 Total Deformation 3 Type: Total Deformation Frequency: 108.7 Hz Unit: mm 11/16/2023 10:06 AM</p> 
W_4	<p>C: Modal test2 Total Deformation 4 Type: Total Deformation Frequency: 122.9 Hz Unit: mm 11/16/2023 10:06 AM</p> 
W_5	<p>C: Modal test2 Total Deformation 6 Type: Total Deformation Frequency: 157.3 Hz Unit: mm 11/16/2023 10:07 AM</p> 

Table 3: Mode shapes from ANSYS

The response of the tip due to the base excitation is obtained using transient structural. The time step used is $1/(20 \cdot \omega)$ which is found in the analysis settings tab and the equivalent damping ratio from modal is set to yes. The details of the Analysis section used to produce the response plots are shown in figure 4 and figure 5.

Details of "Analysis Settings"	
Step Controls	
Number Of Steps	1.
Current Step Number	1.
Step End Time	6. s
Auto Time Stepping	Off
Define By	Time
Time Step	6.107e-004 s
Time Integration	On
Options	
Include Residual Vector	No
On Demand Expansion Option	No
Mode Selection Method	None
Output Controls	
Damping Controls	
Eqv. Damping Ratio From Mo...	Yes
<input type="checkbox"/> Damping Ratio	2.5e-003
Stiffness Coefficient Define By	Direct Input
<input type="checkbox"/> Stiffness Coefficient	0.
<input type="checkbox"/> Mass Coefficient	0.
Numerical Damping	Program Controlled
Numerical Damping Value	0.005
Analysis Data Management	
Visibility	

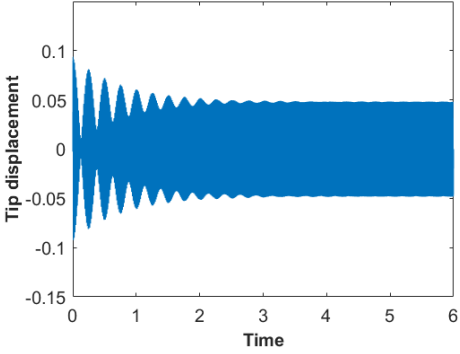
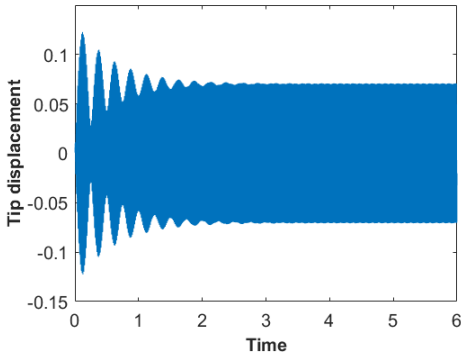
Figure 4: Transient structural analysis settings

Details of "Displacement"	
Scope	
Boundary Condition	Fixed Support
Definition	
Type	Displacement
Absolute Result	Yes
Magnitude	= 0.00001*sin(73.5*360*time)
Direction	Y Axis
Suppressed	No
Function	
Unit System	Metric (m, kg, N, s, V, A) Degrees rad/...
Angular Measure	Degrees
Graph Controls	
Number Of Segments	200.

Figure 5: Transient structural displacement settings

To perform a base excitation in the transient analysis, the modal analysis must be done first, and the solutions shared with the transient analysis. The transient analysis can't be done alone. One of the benefits of ANSYS Transient analysis is that it allows one to provide its own signal / inputs. In displacement tab, base excitation is set to yes and magnitude is $B*\sin(360*w*time)$, w is in hertz. In the solution tab, input the directional deformation along y-axis. The results are shown side by side with the response gotten analytically in table 4.

The results show that the ANSYS and theoretical are in agreement in the steady state response but not the transient response as seen in 77.5Hz, 79.5Hz and 81.5Hz. For the purpose of control system, the steady state is the relevant part.

FREQUENCY	THEORITICAL TIP DISPLACEMENT (mm)	ANSYS TIP DISPLACEMENT (mm)
77.5 Hz		

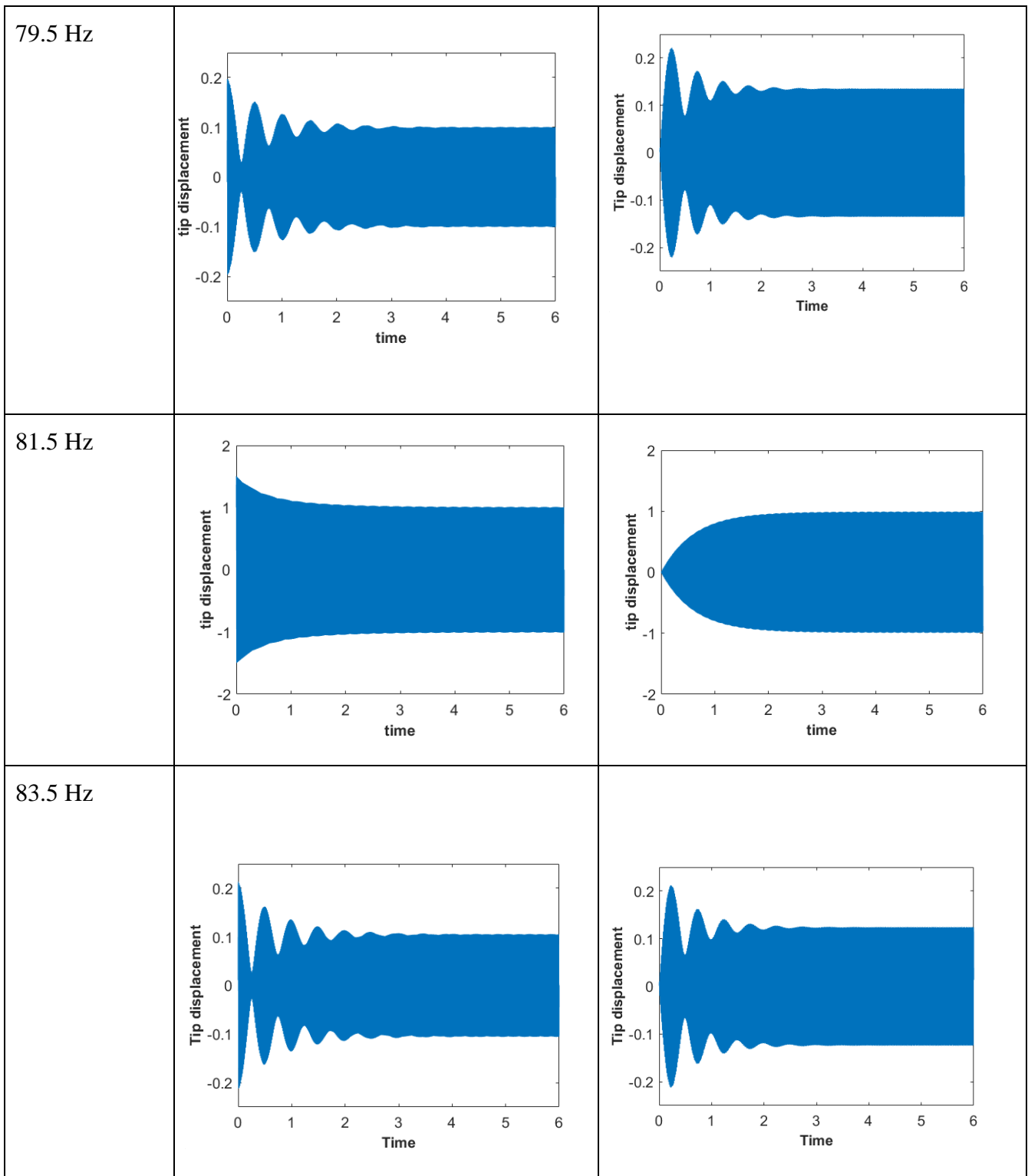


Table 4: Tip displacement responses from transient to steady state for both theoretical and

ANSYS

3.3. Harmonic analysis in ANSYS to get the frequency response function.

A Frequency Response Function (FRF) is a mathematical representation used in engineering and physics to describe the relationship between the input and output of a system subjected to sinusoidal input excitation across a range of frequencies. This is gotten from ANSYS by implementing harmonic analysis. The purpose of generating the FRF is to use it to develop a transfer function within the frequency provided in the harmonic analysis. The key components needed for the TF are the frequency, the amplitude, and the phase. The damping ratio is set to $2.5e-003$, and the solution method is mode superposition which can be done in the analysis settings of the harmonic response as shown in Figure 6.

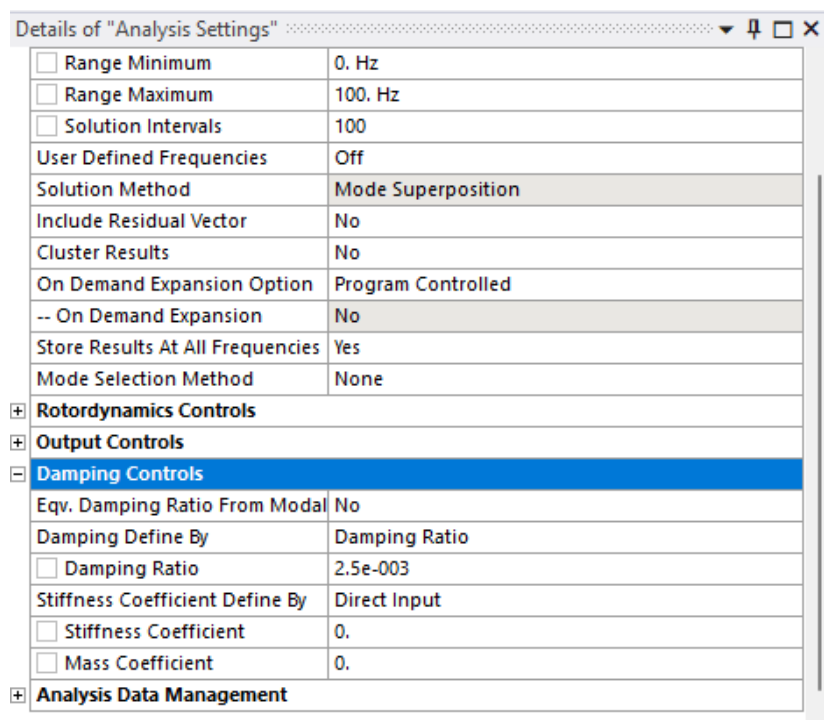


Figure 6: The analysis settings of the harmonic response

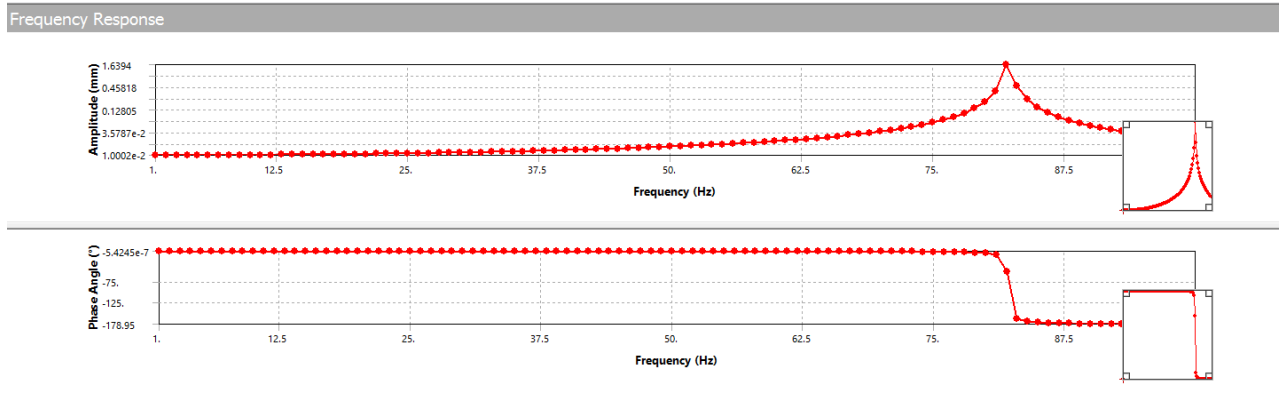


Figure 7: Frequency response plot at tip-mass due to base excitation

3.4. Generate the transfer function based on the Frequency Response Function (FRF) from ANSYS.

System Identification is used to develop the transfer function. Using the system identification toolbox in MATLAB, a fitting transfer function can be found using the frequency, amplitude and phase using the function “tfest”. Before that, the amplitude from ANSYS should be divided by the amplitude of the base displacement which in my case is 0.01mm. Frequency analyzers generally perform this operation before providing the frequency in an experiment. The next step is to create an Iddata object. The MATLAB function for this is ‘idfrd’ in the form “idfrd(amplitude, frequency, sampling time)”.

The transfer function of the cantilever beam with tip-mass is given as:

$$T(s) = \frac{-1.563e06s^2 + 9.757e07s + 9.784e12}{s^4 + 17.03s^3 + 3.698e07s^2 + 9.861e07s + 9.784e12} \quad (4)$$

3.5. Validate the transfer function by comparing the simulated response with the validated response.

MATLAB provides a function called “lsim” to simulate the response of the beam given an input and a transfer function. The transient response from ANSYS is used to validate the response. The ANSYS transient response should match the response simulated by the MATLAB code. The plot in Figure 8 shows both transient responses due to an input of $0.01 \cdot \sin(w \cdot 2 \cdot \pi \cdot t)$ with $w = 10\text{Hz}$. From the plot, the transfer function works well therefore, we can conclude that we understand how to generate a transfer function from ANSYS.

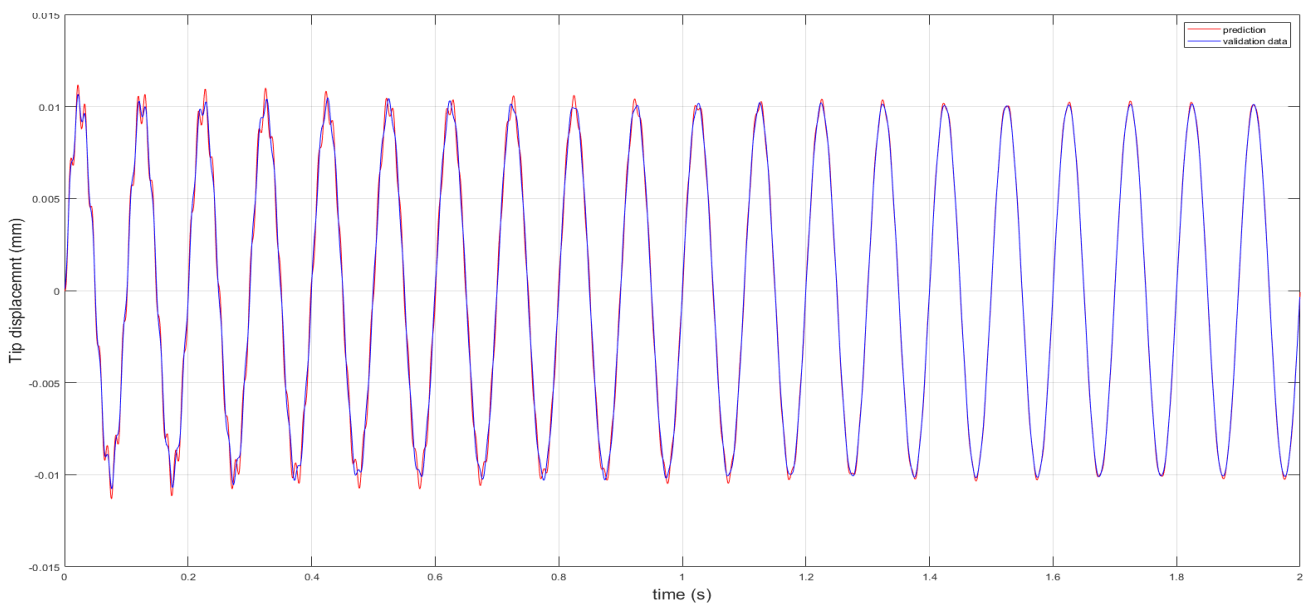


Figure 8: Plot showing the predicted and validation response of the cantilever beam with tip-mass.

CHAPTER 4

4. RESULTS AND DISCUSSIONS

In this chapter, the method used to develop the transfer function of the cantilever with tip-mass is implemented to the camera mount. The modelling of the camera mount correctly is the most important part of this thesis. A cylindrical part was added to the top of the mount to act as the camera as shown in figure 9. The mass of the camera here is 1.1kg changing the first natural frequency of the mount from 500Hz to 325Hz. This natural frequency is ideal because it's far from a typical off-road vibration which varies between 1Hz - 10Hz. The position of the camera is chosen at the top of the mount because the response provided negligible difference compared to if it was positioned below. The negligible difference is because of the rigid body behavior of the camera mount at this camera weight.

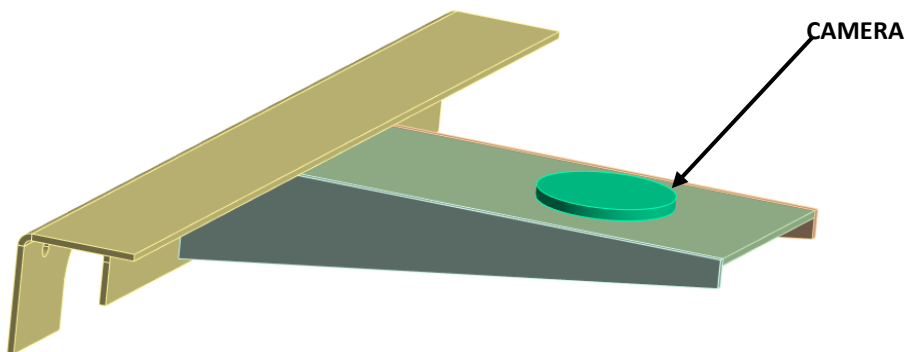


Figure 9: Position of the camera on the camera mount.

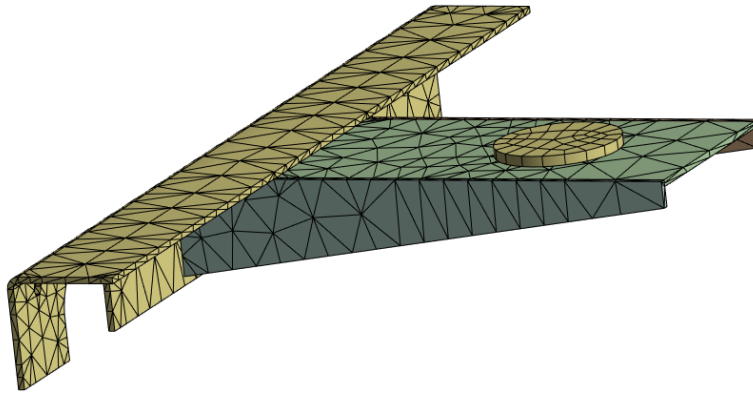


Figure 10: Meshing of the camera mount.

4.1. Mesh Quality

There are several parameters used for meshing quality in ANSYS but we will focus on aspect ratio. Aspect ratio is a measure of the stretching of a cell. It's computed as the ratio of the maximum value to the minimum value of any of the following distances: the distance between the cell centroid and face centroids, and the distance between the cell centroid and nodes. Aspect ratio should ideally be closer to 1.

It is shown in figure 11 that the element size of 10mm (average aspect ratio of 3.9) didn't change the transient response of the system in our situation compared to the transient response using the default mesh of element size of 26.69mm (average aspect ratio of 11.08) so, the default mesh will be used. The default mesh size used has 5420 nodes and 2356 elements shown in figure 10.

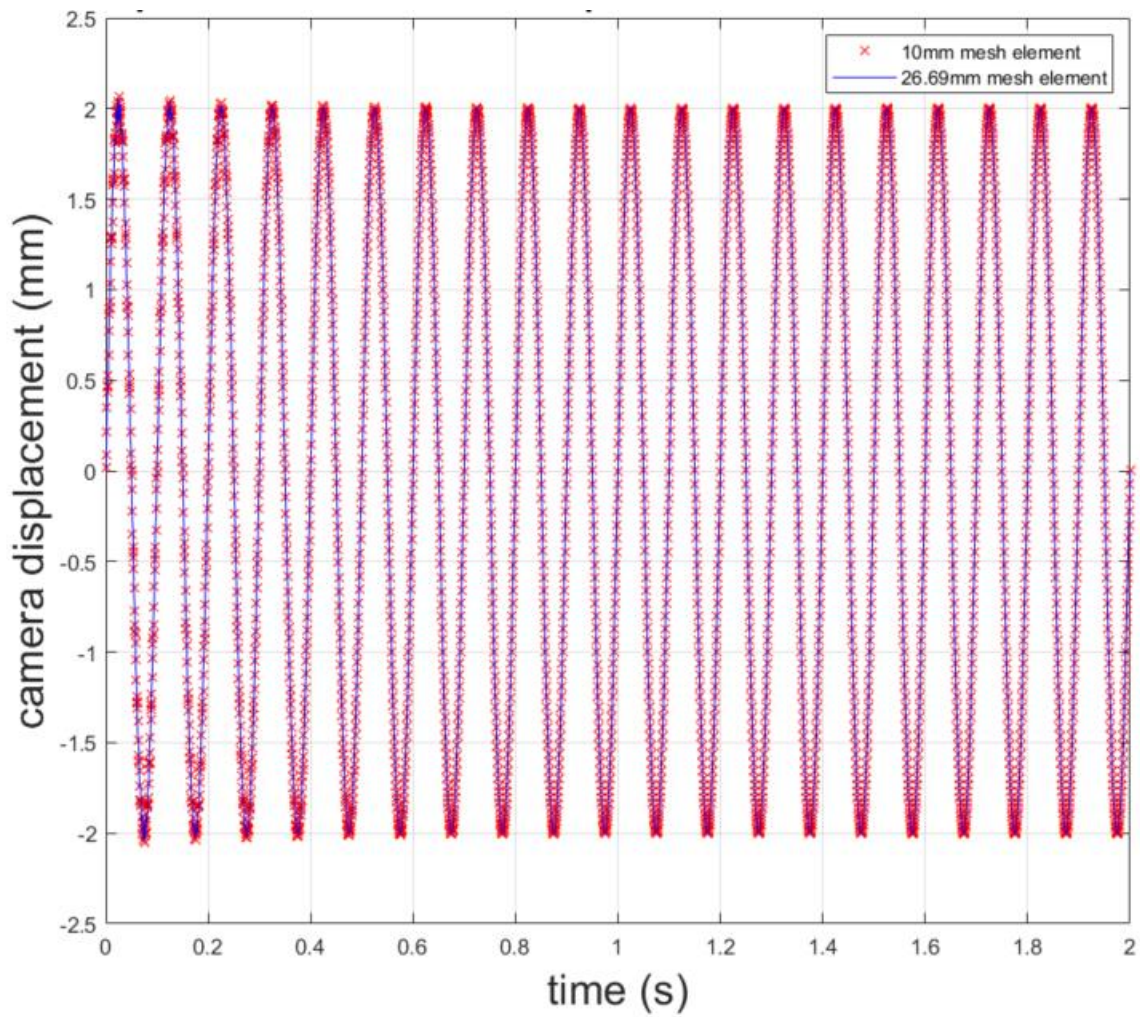


Figure 11: Comparison of the transient responses between two different mesh sizes

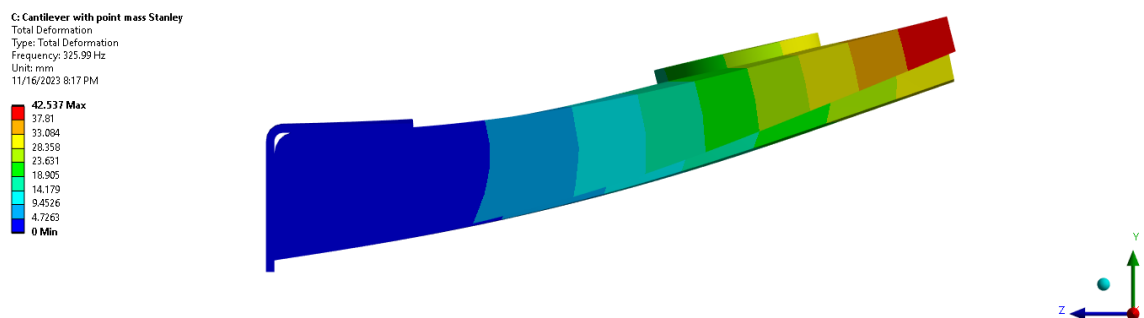


Figure 12: The first mode shape at 325.99Hz

4.2. Frequency Response Function of the Camera Mount

This analysis was conducted by following the methods discussed in Section 3.3 above. A base displacement at the fixed support of a magnitude of 2mm along the y-axis was applied for frequencies ranging from 0 to 3000 Hz to capture the first five natural frequencies which are 325Hz, 1072.6Hz, 1967.3Hz, 2634.2Hz and 2978.6Hz. The reason for the dip in the amplitude and phase shift is due to damping in the system. The FRF plot is show in figure 13.

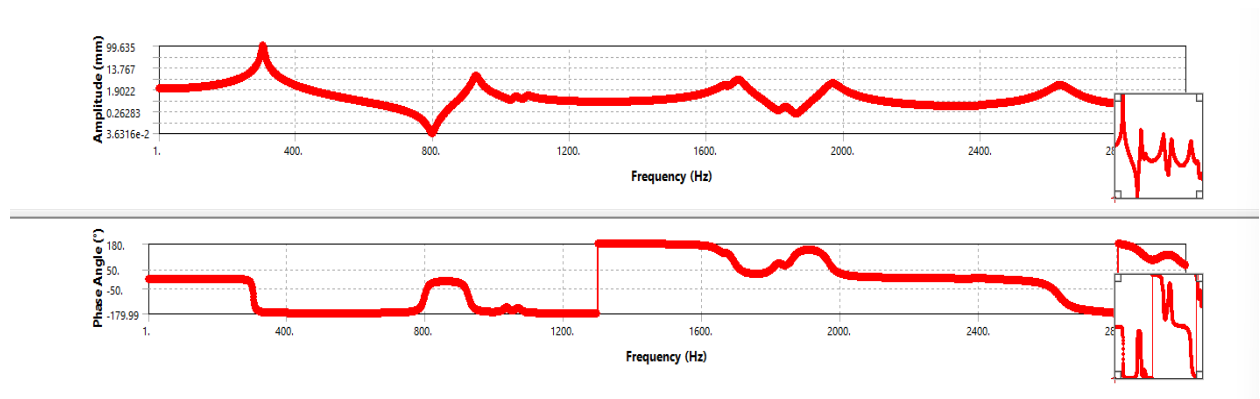


Figure 13: FRF plot at the camera position

4.3. Deriving the Transfer Function using System Identification Toolbox in MATLAB

Using FRF data provided, the transfer function from the base (fixed support) to the position of the camera is obtained as:

$$T(s) = \frac{5.696e06s^2 + 8.955e08 s + 1.321e14}{s^4 + 149.3s^3 + 3.762e07s^2 + 1.706e09s + 1.244e14} \quad (5)$$

4.4. Validation of Derived Transfer Function of Camera Mount

To validate the derived transfer function model, The predicted response using the transfer function is compared to the validation data. The validation is gotten from ANSYS transient response with the input as the same input value provided to the transfer function. Figure 14-17 show the response of comparison between the predicted and validation responses to a sine input.

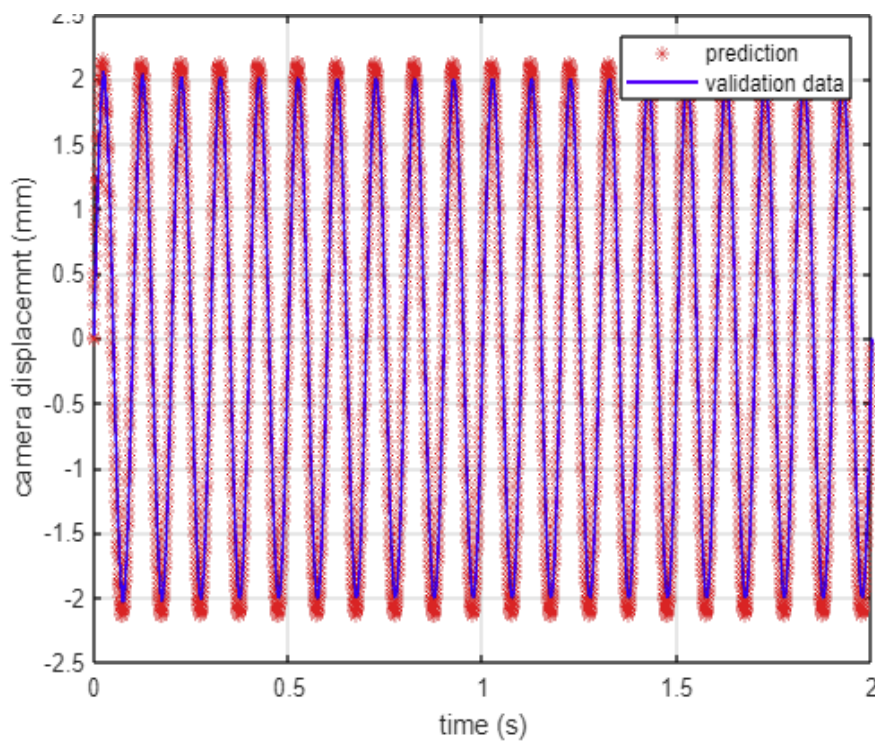


Figure 14: Comparison between FRF transfer function and ANSYS transient simulation (Displacement is 2mm, 10Hz)

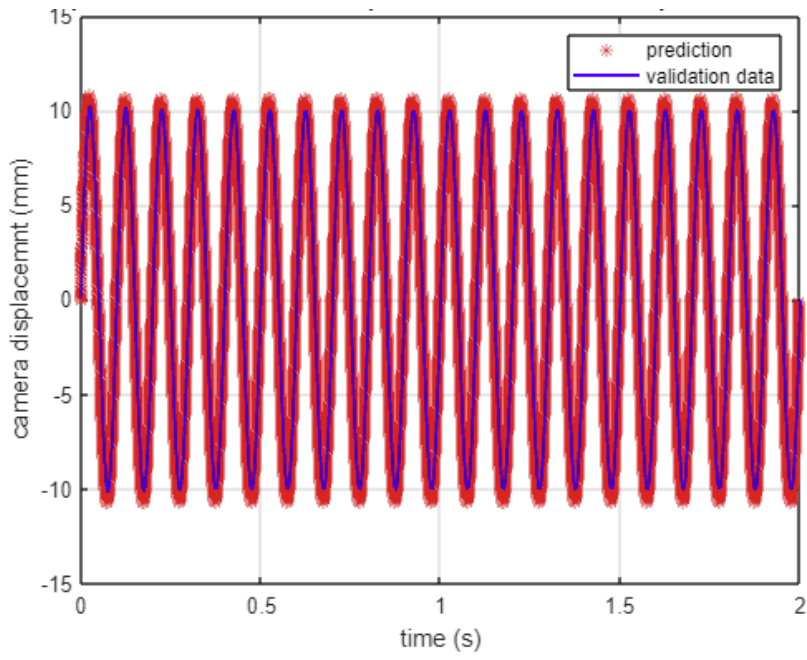


Figure 15: Comparison between FRF transfer function and ANSYS transient simulation (Displacement is 10mm, 10Hz)

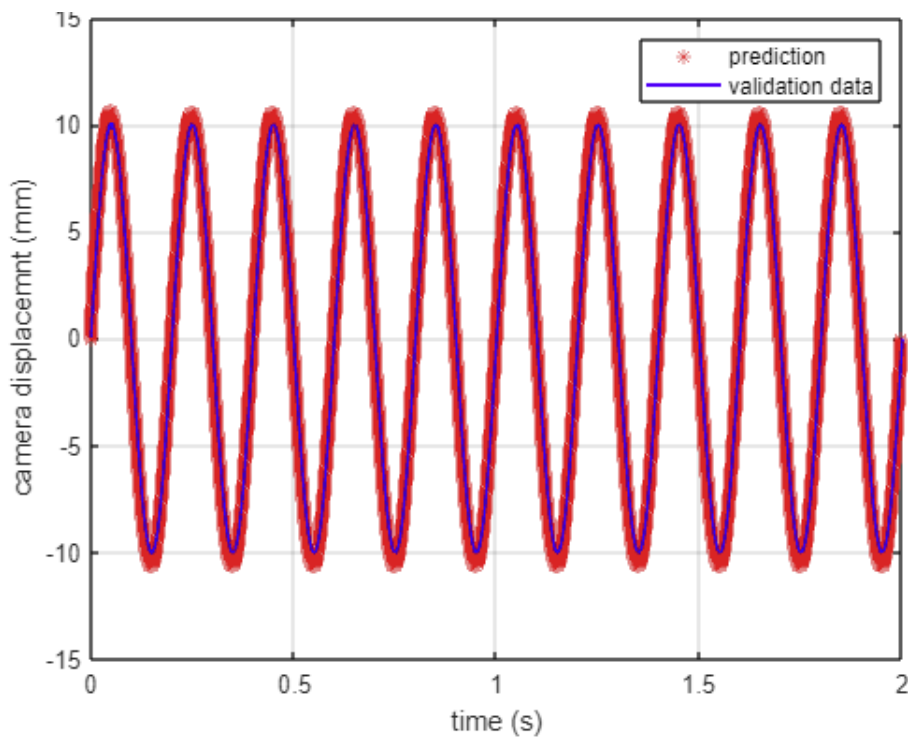


Figure 16: Comparison between FRF transfer function and ANSYS transient simulation (Displacement is 10mm, $\omega = 5\text{Hz}$)

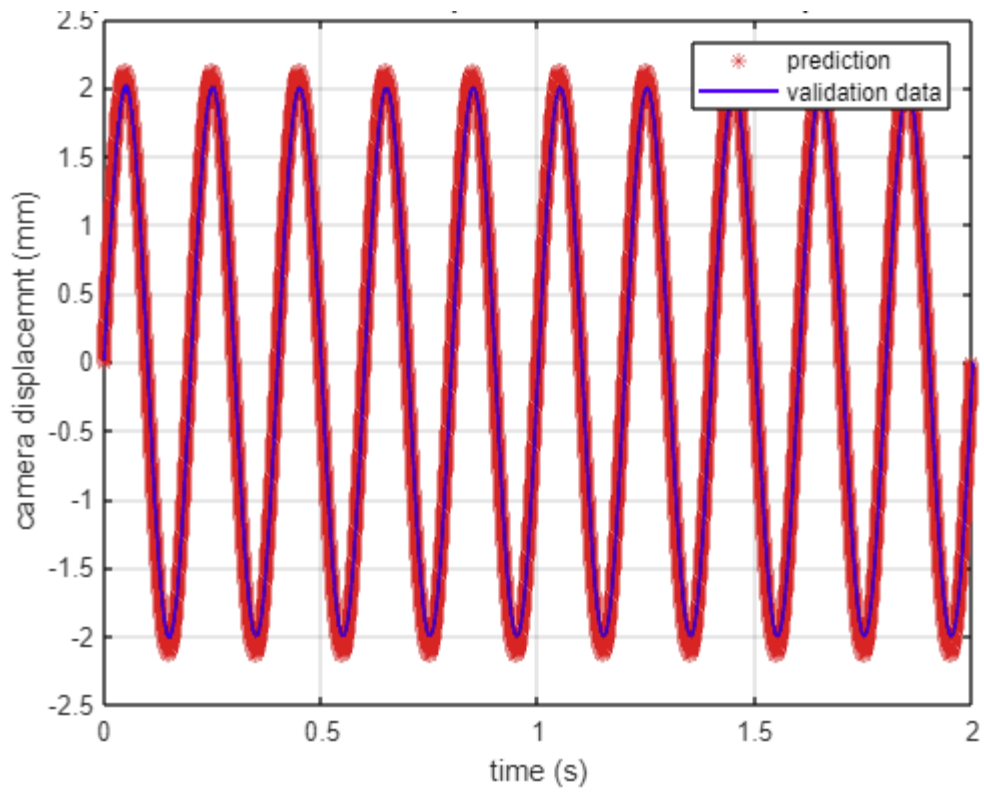


Figure 17: Comparison between FRF transfer function and ANSYS transient simulation (Displacement is 2mm, frequency is 5Hz)

CHAPTER 5

5. CONCLUSION AND RECOMMENDATIONS

This thesis presents a transfer function of a camera mount using ANSYS and MATLAB. It shows the five steps taken to develop the transfer function of the system. Which are to first develop a theoretical response of the structure to base excitation which is then validated with the transient response in ANSYS. A harmonic analysis in ANSYS is done to get the frequency response function. Thereafter, a transfer function is generated by utilizing the System Identification Toolbox in MATLAB, based on the Frequency Response Function (FRF) from ANSYS. Finally, the transfer function is validated by comparing the simulated response to the validated response.

The camera mount is simplified into a cantilever beam with tip-mass and the process developed is then implemented to the camera mount. The transfer function developed in equation 5 predicted the position of the camera mount to an accuracy of 98%. Figure 14-17 show the response of comparison between the predicted and validation responses to a sine input are in agreement.

The rigid body motion observed in figure 14-17 shows that at low frequencies the transfer function is 1. Figure 13 shows that at higher frequencies of 325Hz the camera displacement is about 100mm for a damping of 0.02, meaning it could result in structural failure.

The contribution of this research is that it shows that MATLAB and ANSYS can be used in the development of transfer function for camera mount application. It shows the method of simplifying the complex model to further understand the system and the extraction of the model characteristics for the purpose of transfer function development, crucial to vibration control.

In the future work, this camera mount would include more parts of the assembly as computational power improves with time. Also, the transfer function could be implemented to control the vibration of the camera mount for a HUD application.

Even though the model shows promising results, experimental validation is important. The damping ratio for the actual system is unknown but 0.02 is used for the ANSYS simulations. This procedure could be implemented in situations where the cost of production is high.

6. APPENDIX A

6.1.1. MATLAB codes for obtaining transfer transient response of the cantilever beam

```
clear all;
close all;
clc;
%Define variables
Ls= 10 *10^-3;      %(m)
Lm = 15.6*10^-3;    % length of Tip-mass (m)
tm = 29.5*10^-3;    % Thickness of tip-mass (m)
width = 10.2*10^-3; % (m)
rho_m = 1000; %7753 ; % density of tip-mass (kg/m3)
rho_s = 2630 ; % density of beam (kg/m3)
ts = 4.9*10^-3;    % thickness of beam (m)
B = 0.01*10^-3;    %B, Amplitude of the base vibration (m)
M =Lm*tm*width*rho_m+Ls*ts*width*(rho_s-rho_m); % total mass of tip-mass and
beam (kg)
L = 120.4*10^-3 ;    %L, length of the cantilever beam
r_c = (rho_m*tm*Lm^2 -rho_m*ts*Ls^2 +rho_s*ts*Ls^2)/(2*(rho_m*tm*Lm
+Ls*ts*(rho_s-rho_m))) ; %(m)
%r_c = 0.0602; %testing
J= rho_m*Lm*tm*width*((1/12)*(Lm^2 +tm^2)+((1/2)*Lm -
r_c)^2)+Ls*ts*width*(rho_s-rho_m)*((1/12)*(Ls^2+ts^2) +(r_c-(1/2)*Ls)^2);
m = rho_s*L*ts*width % m, mass of beam (m)
I= (1/12)* width * ts^3 % area moment of inertia
E= 69*10^9; % N/m2
zeta = 0.0025;
phi= M/(rho_s*ts*width*L);
K = sqrt(J/M);
% first five roots (Hz) gotten from roots finder file
w_1 = 81.4764;
w_2 = 912.3990;
w_3 = 2.4790e+03;
w_4 = 5.3576e+03;
w_5 = 9.9459e+03;
```

```

R1 = phi.*u.^3.*((K/L)^2 + (r_c/L)^2) ; %
R2 = phi*u.^2.*(r_c/L); %
A12 = R1.*(cosh(u)-cos(u)) - (1+R2).*sin(u) + (R2 - 1).*sinh(u);
A11 = -(1 + R2).*cos(u)+ (R2 -1).*cosh(u) + R1.*(sin(u) + sinh(u)) ;
lamda = A12./A11;

syms x
U3i = sin(u.*x/L) - sinh(u.*x/L) -lamda.*(cos(u.*x/L)-cosh(u.*x/L));
w_i =[w_1 w_2 w_3 w_4 w_5]*2*pi
w= 85.5*2*pi; %forcing freq
int1 = simplify(int(U3i.^2,x,0,L));
dif1 = simplify(diff(U3i,x));

x_val = 0.1204;
U3i = subs(U3i,x,x_val);
int1 = subs(int1,x,x_val);
dif1 = subs(dif1,x,x_val);

% Norminalized mode shape
delta3i = simplify(sqrt(int1.*m + M.*(U3i).^2 + 2.*r_c.*M.*U3i.*dif1 +
(J+(M.*(r_c.^2))).*(dif1).^2));
%integration and differentitaion using U3in
U3in = simplify(U3i./delta3i);
dif2 = simplify(diff(U3in,x));
int2 = simplify(int(U3in,x,0,L));

% Evaluate U3in, int2, and dif2 at x = 0.1204
U3in = subs(U3in,x,x_val);
int2 = subs(int2,x,x_val);
dif2 = subs(dif2,x,x_val);

phi_1 =atan((2*zeta*sqrt(1-zeta^2))./(w./w_i).^2+2*zeta.^2 -1));
phi_2 = atan(-2*zeta*(w./w_i)/(1-(w./w_i).^2));
% Compute constants for Ut vectorization for quicker processing
const2 =sqrt(w^4 +2*(2*zeta^2 -1)*w^2.*w_i.^2 + w_i.^4);
const1 =w^3./(w_i.*sqrt(1-zeta^2));
%response of the tip mass
x = 0.1204;
syms t
Ut = U3in.*B.*(M.*U3in - r_c.*M.*(dif2) - m.*(int2))./const2 .*(const1...
.*exp(-w_i.*zeta.*t).*sin(w_i.*sqrt(1-zeta.^2).*t+phi_1)+w.^2.*sin(w.*t +
phi_2));
Ut1 = Ut(:,1);
Ut2 = Ut(:,2);
Ut3 = Ut(:,3);
Ut4 = Ut(:,4);
Ut5 = Ut(:,5);
Uat = (Ut1 + Ut2 + Ut3 + Ut4 + Ut5)*1000;

t_val= linspace(0, 6, w*20);
Uat = subs(Uat, t,t_val);

```

```

figure
plot(t_val,Uat);
xlim([0 6]);
%ylim([-5e-5 5e-5]);
xlabel('t');
ylabel('tip displacement')

```

6.1.2. Root finder MATLAB code

```

syms u
N =50;
u =linspace(-10,15,N);
%The characteristic equation to obtain wn= 81.5Hz
D = cos(u).*cosh(u) + (4813758662050123.*u.*(cos(u).*sinh(u) -
cosh(u).*sin(u)))/2251799813685248 -
(15562404948525407075412203067517.*u.^3.*(cos(u).*sinh(u) + cosh(u).*sin(u) +
(4813758662050123.*u.*(cos(u).*cosh(u) -
1))/2251799813685248))/649037107316853453566312041152512 +
(133194714419274746521393181085894027478080985738498388175646225.*u.^4.*(cos(u)
).*cosh(u) -
1))/6582018229284824168619876730229402019930943462534319453394436096 -
(11541001447849954520921166920215.*u.^2.*sin(u).*sinh(u))/40564819207303340847
894502572032 + 1;
%Plot graph
plot(u,D);
xlim([0 15]);
ylim([-0.5 0.5])
hold on
% Plot the horizontal line
plot(u, zeros(size(u)), 'k-');
xlabel('u');
ylabel('D');
title('curve of u against D');
hold off
% Insert your guess of u based on the plot
f= @(u) cos(u).*cosh(u) + (4813758662050123.*u.*(cos(u).*sinh(u) -
cosh(u).*sin(u)))/2251799813685248 -
(15562404948525407075412203067517.*u.^3.*(cos(u).*sinh(u) + cosh(u).*sin(u) +
(4813758662050123.*u.*(cos(u).*cosh(u) -
1))/2251799813685248))/649037107316853453566312041152512 +

```

```

(133194714419274746521393181085894027478080985738498388175646225.*u.^4.*(cos(u)
).*cosh(u) -
1))/6582018229284824168619876730229402019930943462534319453394436096 -
(11541001447849954520921166920215.*u.^2.*sin(u).*sinh(u))/40564819207303340847
894502572032 + 1;

% Find the root
x0 =5; % Starting guess %use the plot above to make a guess of x0
x = fzero(f, x0);

% Display the result
fprintf('The root is approximately %f.\n', x);

```

6.2. MATLAB codes for obtaining transfer function of the cantilever beam with tip-mass

```

clear all; close all; clc;
load('lowfreq')
Fbeam1= 0.01;
Freq3=Ansysfrf_beam(:,1);
W3=2*pi*Freq3;
Amp3=Ansysfrf_beam(:,2)/Fbeam1;
Pha3=Ansysfrf_beam(:,3);
zfr3 =Amp3.*exp(1i*Pha3*pi/180); %in complex form
Ts =0;
gfr3 = idfrd(zfr3,W3,Ts);
np3 = 4;
nz3 = 2;
sys3 = tfest(gfr3,np3,nz3)

t1=0:0.1e-04:2; %sampling time affects the response
w=10;
Ubeam1 =Fbeam1*sin(w*2*pi*t1); % base excitation displacement
Ybeam1 = lsim(sys3,Ubeam1,t1); % simulated tip displacement from TF

tt1=AnsysTrans_beam(:,1); %time from ANSYS transient analysis
Yansys1=AnsysTrans_beam(:,2); % tip displacement from transient analysis.
plot(t1,Ybeam1,'r',tt1,Yansys1,'b')
legend('prediction','validation data')
grid on

```

```

ylabel('Tip displacemnt (mm)','FontSize',20)
xlabel('time (s)','FontSize',20)
title('Comparison of Validation Response and Predicted Response for
Cantilever Beam with Tip-Mass','FontSize',16)

```

6.3. MATLAB codes for obtaining transfer function of the camera mount using ANSYS FRF data.

```

clear all;
load('Ansyscamera') %frf and transient response from ANSYS
Disp= 2; %input displacement
Freq=frf_camera(:,1);
W=2*pi*Freq;
Amp=frf_camera(:,2)/Disp;
Pha=frf_camera(:,3);
zfr =Amp.*exp(1i*Pha*pi/180); %in complex form
Ts =0;

gfr = idfrd(zfr,W,Ts) %creates iddata
np = 4; %number of poles
nz = 2; %number of zeros

sys = tfest(gfr,np,nz) %Transfer function of the camera mount
t1=0:6.107e-004:2; %sampling time affects the response
w= 10; %hz forcing freq
Ubeam = Disp*sin(w*2*pi*t1); % Input harmonic displacement
Ybeam = lsim(sys,Ubeam,t1); % Output displacement using the transfer
function
tt=trans_camera(:,1);
Yansys=trans_camera(:,2);
plot(t1,Ybeam,'r*',tt,Yansys,'b')
legend('prediction','validation data')
grid on
ylabel('camera displacemnt (mm)')
xlabel('time (s)')

title('Comparision of Validation Response and Predicted Response for
Camera')

```

7. APPENDIX B

This is the documentation of the functions used in the system ID toolbox.

“**tfest**” is used to estimate transfer function using time or frequency domain data.

Construction:

```
SYS = tfest(DATA, NP, NZ)
```

uses NZ number of zeros for estimation of transfer function SYS. For continuous-time models, NZ must be less than or equal to NP (unless continuous-time data is used). In discrete-time case, choose "NZ" to be the number of zeros of the numerator polynomial in z^{-1} variable.

“**idfrd**” is used to construct or convert to Identified Frequency Response Data model.

Identified Frequency Response Data (idfrd) models are useful for storing frequency responses of linear systems as well as their uncertainties. idfrd also stores experimental response data, and directly estimated frequency responses obtained from SPA, SPAFDR and ETFE. Parts of the response can be selected by FSELECT.

Construction:

```
MF = idfrd(RESPONSE,FREQS,TS)
```

 creates an idfrd model MF with response data in RESPONSE at frequency points in FREQS. The output SYS is an object of class @idfrd. TS is the sample time. Use TS = 0 to denote the response from a continuous time system.

“**Lsim**” is used to simulate time response of dynamic systems to arbitrary inputs.

Construction:

$Y = \text{lsim}(\text{SYS}, U, T)$

computes the response Y of the dynamic system SYS to the input signal described by U and T . The time vector T is expressed in the time units of SYS and consists of regularly spaced time samples. The matrix U has as many columns as inputs in SYS and $U(i,:)$ specifies the input value at time $T(i)$. For example,

$t = 0:0.01:5; \quad u = \sin(t); \quad \text{lsim}(\text{sys}, u, t)$

simulates the response of a single-input model SYS to the input $u(t)=\sin(t)$ during 5 time units.

REFERENCES

- Pauzie. (2015). Head-up display in automotive: A new reality for the driver. In Proc. 4th Int. Conf. Design, User Expert., Usability, Los Angeles, CA, USA (pp. 505–516).
- Ablaßmeier, M., et al. (2007). Eye gaze studies comparing head-up and head-down displays in vehicles. *IEEE International Conference on Multimedia and Expo*, 2250-2252.
- Kim, S., & Dey, A. (2009). Simulated augmented reality windshield display as a cognitive mapping aid for elder driver navigation. *Proceedings of the SIGCHI Conference on Human Factors in Computing Systems*, 133-142.
- Medenica, Z., Kun, A. L., Paek, T., & Palinko, O. (2011). Augmented reality vs street views: A driving simulator study comparing two emerging navigation aids. *Proceedings of the 13th International Conference on HCI with Mobile Devices and Services*, 265-274.
- Jaiswal, S., Aman, R., Sapanen, J., & Mikkola, A. (2021). Real-time multibody model-based heads-up display unit of a tractor. *IEEE Access*, 9, 57645-57657. DOI: 10.1109/ACCESS.2021.3072452
- Hasegawa, T., Sumiyosi, Y., Hayashi, Y., Nishikawa, A., Chikuri, T., & Tsukahara, O. (2019). Position correction against vehicle vibration for augmented reality on head-up display. In *SID Symposium Digest of Technical Papers*, San Jose, CA, USA (pp. 1404–1407).
- Bozhevolnyi, S. I., Vohnsen, B., & Bozhevolnaya, E. A. (1999). Transfer functions in collection scanning near-field optical microscopy. *Optics communications*, 172(1-6), 171-179.

- Chu, M., Matthews, J., & Love, P. E. (2018). Integrating mobile building information modelling and augmented reality systems: an experimental study. *Automation in Construction*, 85, 305-316.
- Datcu, S., Ibos, L., Candau, Y., & Matteï, S. (2002). *On the FPA infrared camera transfer function calculation*. Paper presented at the Proc. of the 6th Int. Conf. on Quantitative InfraRed Thermography.
- Friedrich, D., Brauers, J., Bell, A. A., & Aach, T. (2010). *Towards fully automated precise measurement of camera transfer functions*. Paper presented at the 2010 IEEE Southwest Symposium on Image Analysis & Interpretation (SSIAI).
- Haidegger, T., Kovács, L., Precup, R.-E., Benyó, B., Benyó, Z., & Preitl, S. (2012). Simulation and control for telerobots in space medicine. *Acta Astronautica*, 81(1), 390-402.
- Hilkert, J. (2008). Inertially stabilized platform technology concepts and principles. *IEEE control systems magazine*, 28(1), 26-46.
- Hussain, K., & Kaptan, V. (2004). Modeling and simulation with augmented reality. *RAIRO-Operations Research*, 38(2), 89-103.
- Khot, S., & Yelve, N. P. (2011). Modeling and response analysis of dynamic systems by using ANSYS© and MATLAB©. *Journal of Vibration and Control*, 17(6), 953-958.
- Lepetit, V., Vacchetti, L., Thalmann, D., & Fua, P. (2003). *Fully automated and stable registration for augmented reality applications*. Paper presented at the The Second IEEE and ACM International Symposium on Mixed and Augmented Reality, 2003. Proceedings.
- Ligorio, G., & Sabatini, A. M. (2015). A simulation environment for benchmarking sensor fusion-based pose estimators. *Sensors*, 15(12), 32031-32044.

- López-Mendoza, D., Connolly, D. P., Romero, A., Kouroussis, G., & Galvín, P. (2020). A transfer function method to predict building vibration and its application to railway defects. *Construction and building materials*, 232, 117217.
- Piriadarshani, D., & Sujitha, S. S. (2018). The role of transfer function in the study of stability analysis of feedback control system with delay. *International Journal of Applied Mathematics*, 31(6), 727.
- Sarwar, I. S., & Malik, A. M. (2010). Stability analysis and simulation of a two DOF robotic system based on linear control system. *International journal of intelligent systems technologies and applications*, 8(1-4), 3-17.
- Sırakaya, M., & Alsancak Sırakaya, D. (2022). Augmented reality in STEM education: A systematic review. *Interactive Learning Environments*, 30(8), 1556-1569.
- Syed, T. A., Siddiqui, M. S., Abdullah, H. B., Jan, S., Namoun, A., Alzahrani, A., . . . Alkhodre, A. B. (2022). In-depth review of augmented reality: Tracking technologies, development tools, AR displays, collaborative AR, and security concerns. *Sensors*, 23(1), 146.
- Wu, X. F., Lei, Y. J., Li, D. K., & Xie, Y. (2013). Transfer function modeling of structural vibration of complex aerospace structures based on finite element analysis. *Journal of Mechanical Science and Technology*, 27, 1245-1253.
- Wang, H., Qingfeng, M., & Wuwei, F. (2014). Discussion of the improved methods for analyzing a cantilever beam carrying a tip-mass under base excitation. *Shock and Vibration*, 2014.
- Mendoza-Ramírez, C. E., Tudon-Martínez, J. C., Félix-Herrán, L. C., Lozoya-Santos, J. de J., & Vargas-Martínez, A. (2023). Augmented Reality: Survey. *Applied Sciences*, 13(18), 10491. <https://doi.org/10.3390/app131810491>

Warren, C. (2014). MATLAB for Engineers: Development of an Online, Interactive, Self-study Course. *Engineering Education*, 9(1), 86–93.

<https://doi.org/10.11120/ened.2014.00026>

Mohanty, B. P., & Goswami, L. (2021). Advancements in augmented reality. *Materials Today: Proceedings*.

Radeş, M. (2001). COMPARISON OF VIBRATION PROPERTIES | Comparison of Response Properties. *Encyclopedia of Vibration*, 272–277.

<https://doi.org/10.1006/rwvb.2001.0175>

(2023). 2017 Jeep Wrangler [photograph]. cars.com. <https://www.cars.com/research/jeep-wrangler-2017/>